

ORIGINAL PAGE IS  
OF POOR QUALITY

N 84 20547 D22

## MODELING OF DILUTION JET FLOWFIELDS

by J.D. Holdeman  
NASA Lewis Research Center

and

R. Srinivasan  
The Garrett Turbine Engine Company

Considerations of dilution zone mixing in gas turbine combustion chambers have motivated several studies of the mixing characteristics of a row of jets injected normally into a flow of a different temperature in a constant area duct.<sup>1-4</sup> Recently, experiments have been performed to extend these investigations to include geometric and flow variations characteristic of most gas turbine combustion chambers, namely a variable temperature mainstream, flow area convergence, and opposed rows of jets, either in-line or staggered;<sup>5-7</sup> see figures 1 & 2.

The present paper will compare temperature field measurements from selected cases in these investigations with distributions calculated with an empirical model based on assumed vertical profile similarity and superposition<sup>8</sup> and with a 3-D elliptic code using a standard K-E turbulence model.<sup>9</sup> The results will show the capability (or lack thereof) of the models to predict the effects of the principle flow and geometric variables.<sup>1-4,6,7</sup>

Variations with Orifice Size and Spacing. At constant orifice area, changes in orifice size and spacing can result in jets which vary from under-penetration to over-penetration. This is shown in figure 3a) and b), for jets from closely spaced small orifices and widely spaced larger orifices respectively. The empirical model reproduces the data very well in the small orifice case, since the data are consistent with the major assumption in the empirical model, that all vertical temperature distributions can be reduced to similar Gaussian profiles. The empirical model does not do as well in the larger orifice case however, as the jets have impinged on the opposite wall and the vertical profiles are not similar.

The analytical model calculations made with approximately 20,000 nodes, although in qualitative agreement with the data, under-predict the mixing. That is, the temperature gradients, especially in the transverse direction, are too steep. This result is typical of the analytical model calculations to be shown in this paper. For the small-orifice case a coarse-grid calculation using less than 6000 nodes was also performed. This solution illustrates the diffusive nature of the calculation

ORIGINAL PAGE IS  
OF POOR QUALITY

and the significant influence of grid selection on the solution obtained.

Coupled Spacing and Momentum Flux Ratio. Examination of the experimental data revealed that similar profiles can be obtained over a range of momentum flux ratios, independent of orifice diameter, if orifice spacing and momentum flux ratio are correctly coupled.<sup>1,4,5,7</sup> This is shown in figure 4a) to c).

In all of the combinations shown here, the empirical model results are in very good agreement with the data, as the data are consistent with the Gaussian profile assumption. The analytical model calculations using approximately 20,000 nodes for these cases agree qualitatively with the data, as in the previous figure. In the medium momentum flux ratio case, a second calculation was performed with the same total number of grid points, but with the nodes slightly more concentrated in the vicinity of the jet exit. As can be seen in figure 4b), these two results are not substantially different.

Variable Temperature Mainstream. The influence of a non-isothermal mainstream flow on the profiles for medium momentum flux ratios with  $S/Ho=.5$  and  $Ho/D=4$  can be seen by comparing figures 5 & 6. The shape of the experimental profiles in figure 6 suggests modeling them as a superposition of the upstream profile and the corresponding jets-in-an-isothermal mainstream distribution.<sup>7</sup> This gives only a crude approximation however, as seen in the empirical model results, because of the cross-stream transport of mainstream fluid due to the blockage, which is not accounted for in superimposing the distributions.

In the variable temperature mainstream case the analytical model results agree well with the experimental data, especially on the jet centerplane, but the transverse mixing is underpredicted, as in the corresponding isothermal mainstream case in figure 5.

Opposed Rows of In-line Jets. For opposed rows of jets, with the orifice centerlines in-line, the optimum ratio of orifice spacing to duct height is one-half of the optimum value for single-side injection at the same momentum flux ratio.<sup>7</sup> As an example consider the single-side case with  $S/Ho=.5$  and  $Ho/D=4$  in figure 5 and the opposed row of in-line jets with  $S/Ho=.25$  and  $Ho/D=8$  in figure 7.

The empirical model predicts the opposed-jet case very well, verifying the primary assumption that the effect of a plane of symmetry is similar to that of an opposite wall.<sup>6,7</sup> Note that the experimental profiles on both sides of the plane of symmetry support the Gaussian profile assumption. The analytical model results show the steep transverse and lateral gradients seen in almost all of the previous calculations also,

but are in otherwise good agreement with the data.

Opposed Rows of Staggered Jets. For opposed rows of jets, with the orifice centerlines staggered, the optimum ratio of orifice spacing to duct height is double the optimum value for single-side injection at the same momentum flux ratio.<sup>7</sup> As an example consider the single-side case with  $S/H_0=.5$  in figure 5, and the opposed row of staggered-jets with  $S/H_0=1$  in figure 8.

The empirical model does not handle this complex case well, as the fluid dynamic interactions here are not amenable to a direct extension of the simple Gaussian profile and superposition type modeling appropriate for most of the single-side and opposed-jet cases of interest. The analytical model calculations give slightly better agreement with the data than does the empirical model, and would be expected to improve with overall improvements in the capability of the 3-D codes.

#### REFERENCES

1. Walker, R.E. and Kors, D.L.: Multiple Jet Study Final Report. NASA CR-121217, 1973.
2. Holdeman, J.D., Walker, R.E., and Kors, D.L.: Mixing of Multiple Dilution Jets with a Hot Primary Airstream for Gas Turbine Combustors. AIAA Paper 73-1249, 1973.
3. Walker, R.E. and Eberhard, R.G.: Multiple Jet Study Data Correlations. NASA CR-134796, 1975.
4. Holdeman, J.D. and Walker, R.E.: Mixing of a Row of Jets with a Confined Crossflow. AIAA Journal, vol.15, no.2, Feb.1977, pp243-249.
5. Srinivasan, R., Berenfeld, A., and Mongia, H.C.: Dilution Jet Mixing Program - Phase I Report. NASA CR-168031, 1982.
6. Srinivasan, R., Coleman, E., Johnson, K., and Mongia, H. C.: Dilution Jet Mixing Program - Phase II Report. NASA CR-174624, 1984.
7. Srinivasan, R., Reynolds, R., Ball, I., Berry, R., Johnson, K., and Mongia, H.: Aerothermal Modeling Program - Phase I Final Report. NASA CR-168243, 1983.
8. Holdeman, J.D.: Perspectives on the Mixing of a Row of Jets with a Confined Crossflow. AIAA-83-1200, 1983.
9. Holdeman, J.D., Srinivasan, R., and Berenfeld, A.: Experiments in Dilution Jet Mixing. AIAA-83-1201, 1983.

ORIGINAL PAGE IS  
OF POOR QUALITY

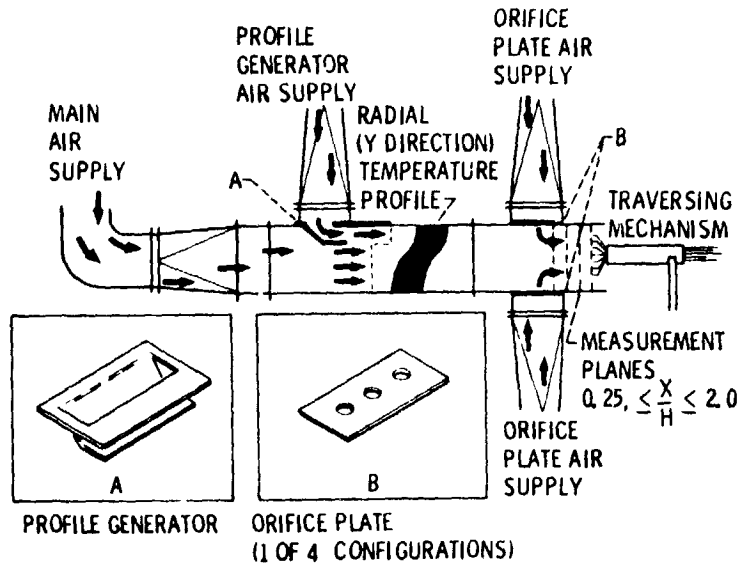


Figure 1. - Dilution Jet Mixing Flow Schematic.

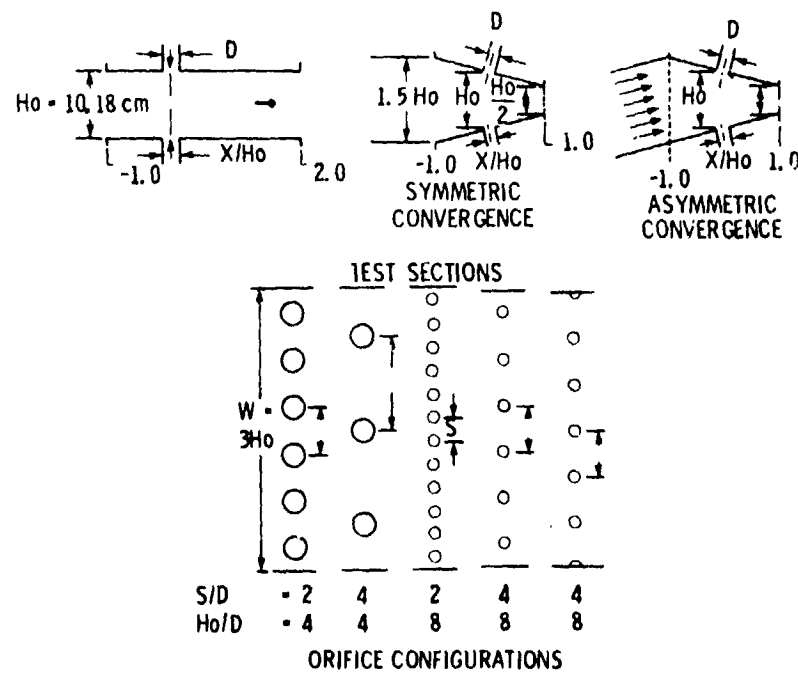
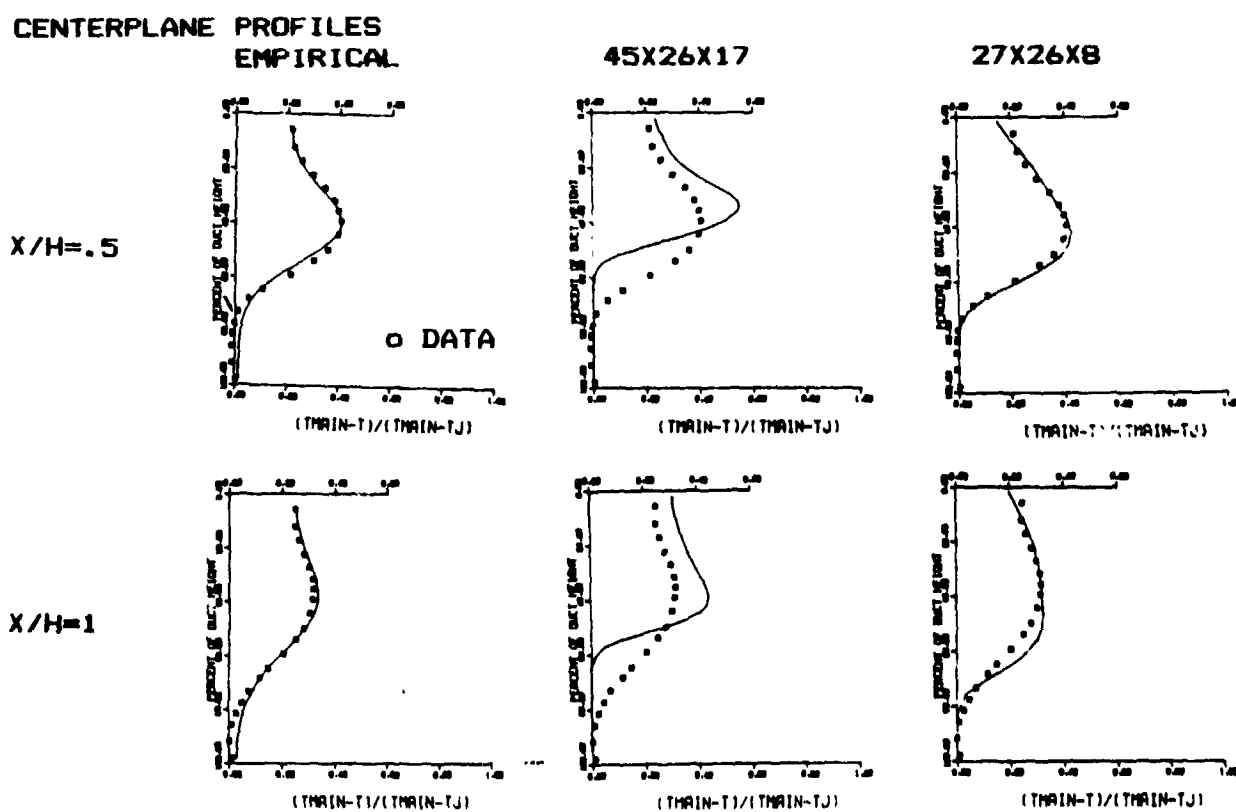
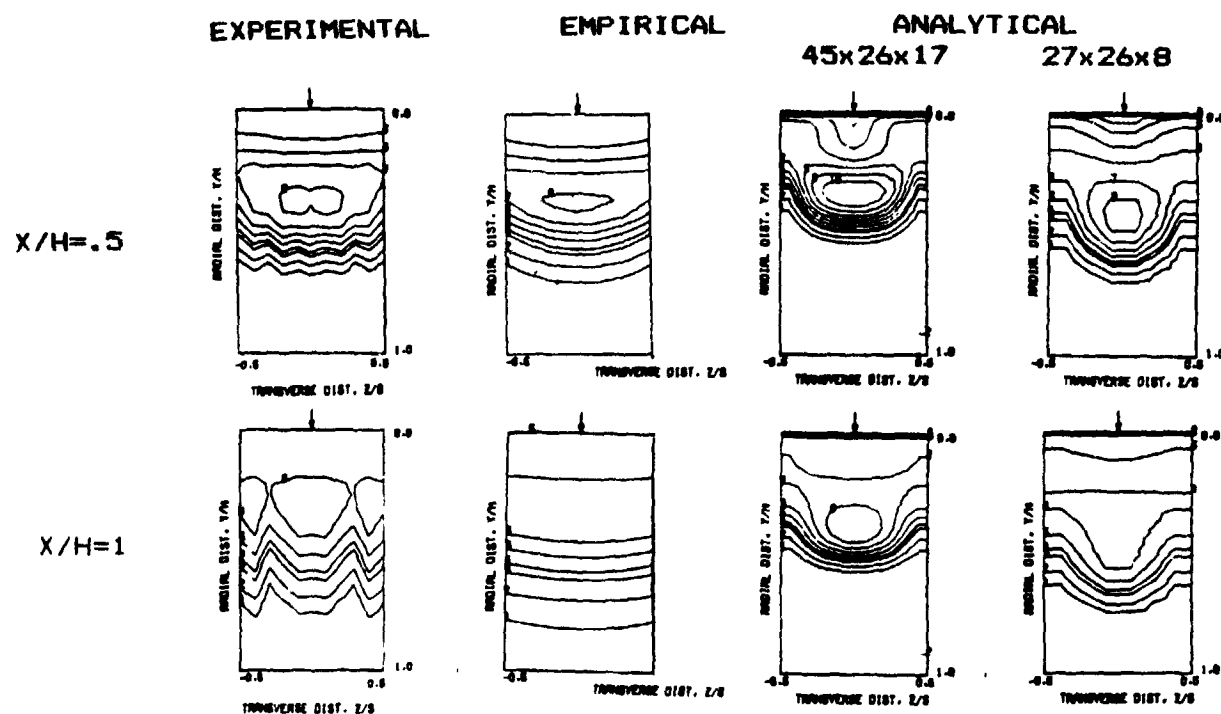


Figure 2. - Test Sections and Orifice Configurations.

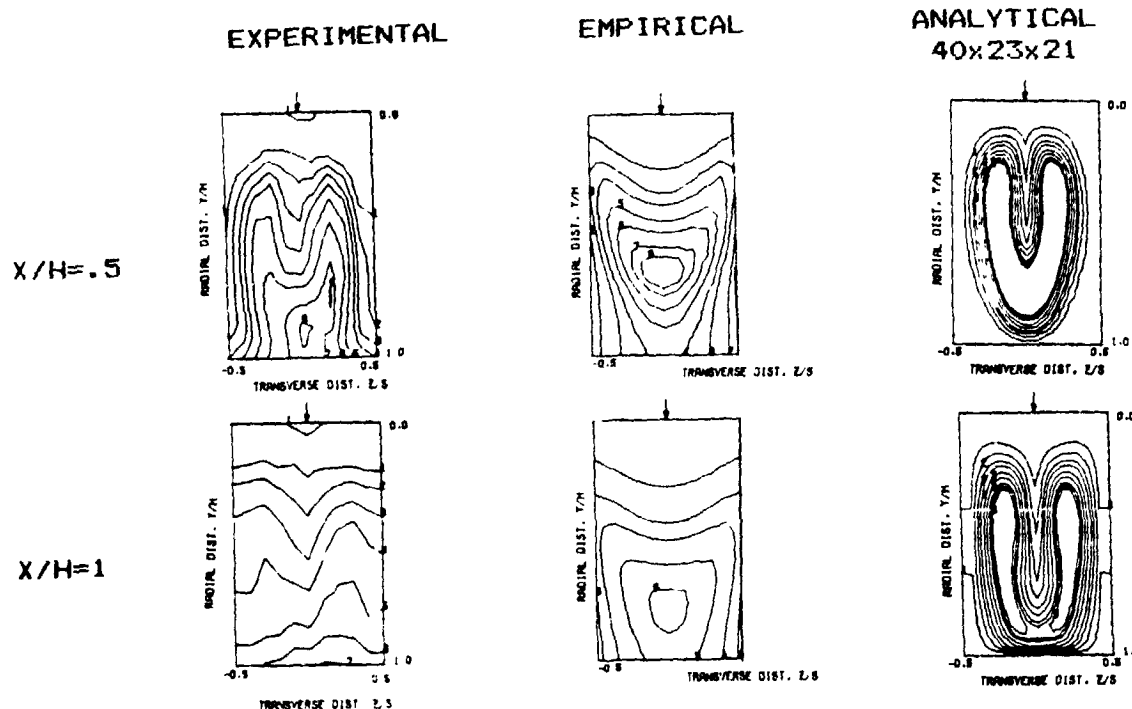
ORIGINAL PAGE IS  
OF POOR QUALITY



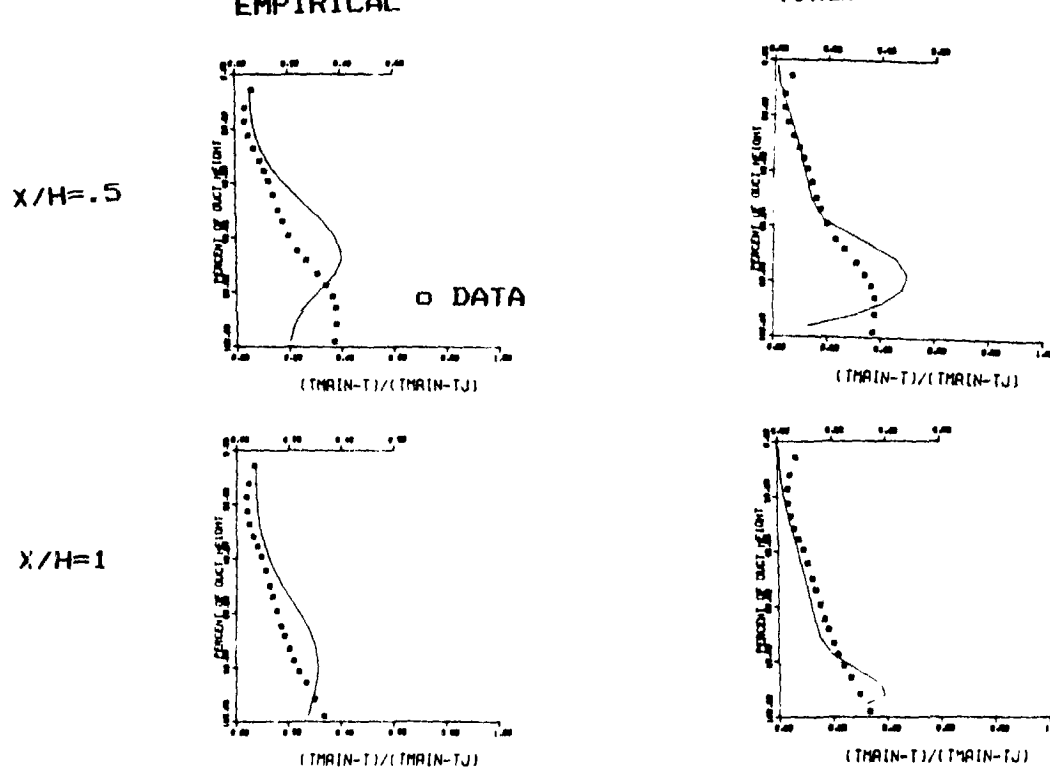
a)  $S/H_0 = .25$ ,  $H_0/D = 8$ ,  $A_s/A_m = .049$ ,  $J = 25.3$ ,  $W_s/W_t = .169$

Figure 3. Effect of Variations in Orifice Size and Spacing on Temperature Distributions

ORIGINAL PAGE IS  
OF POOR QUALITY



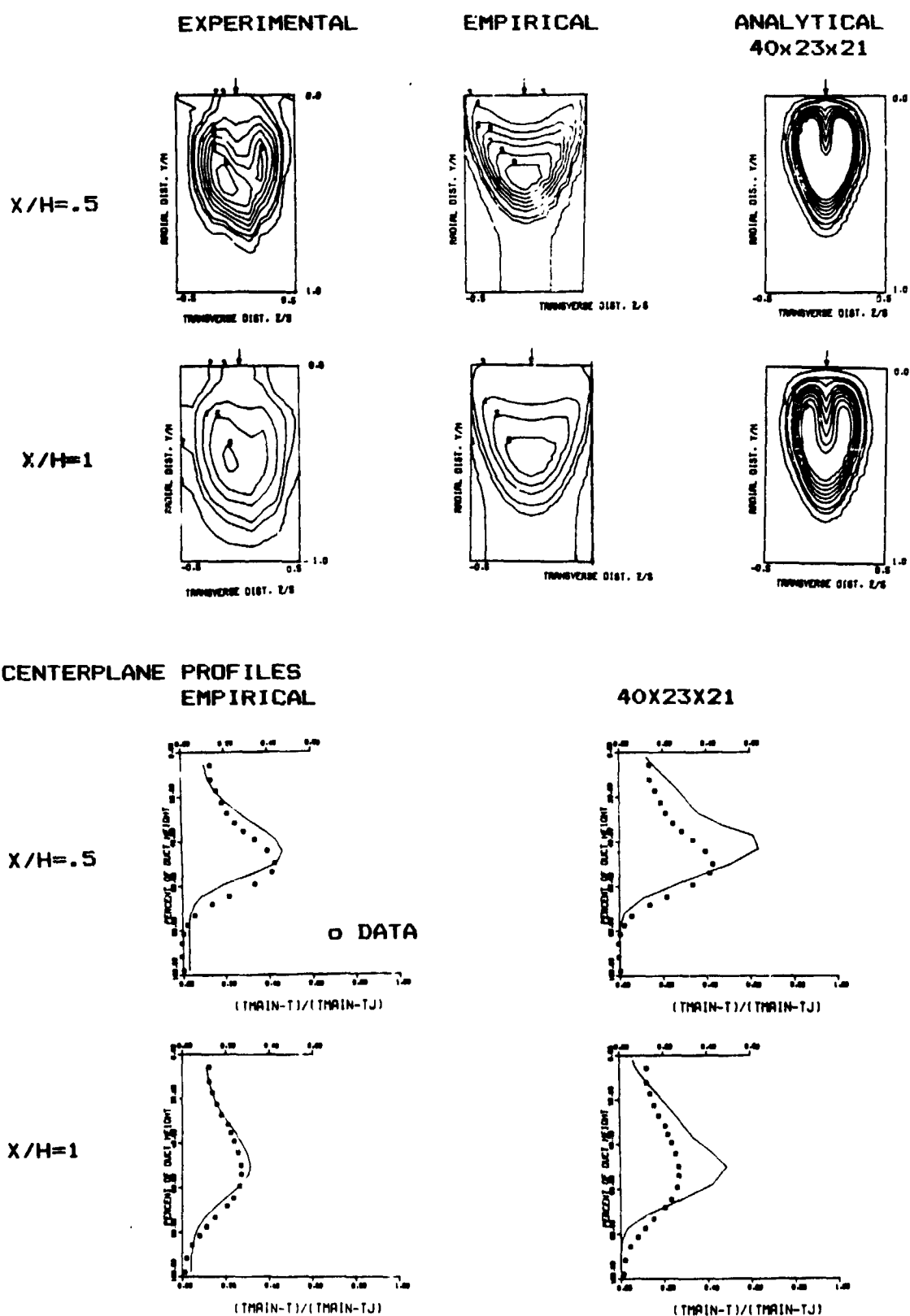
CENTERPLANE PROFILES  
EMPIRICAL



b)  $S/H_0=1$ ,  $H_0/D=4$ ,  $A_s/A_m=.049$ ,  $J=26.7$ ,  $w_j/w_T=.192$

Figure 3. Effect of Variations in Orifice Size and Spacing on Temperature Distributions

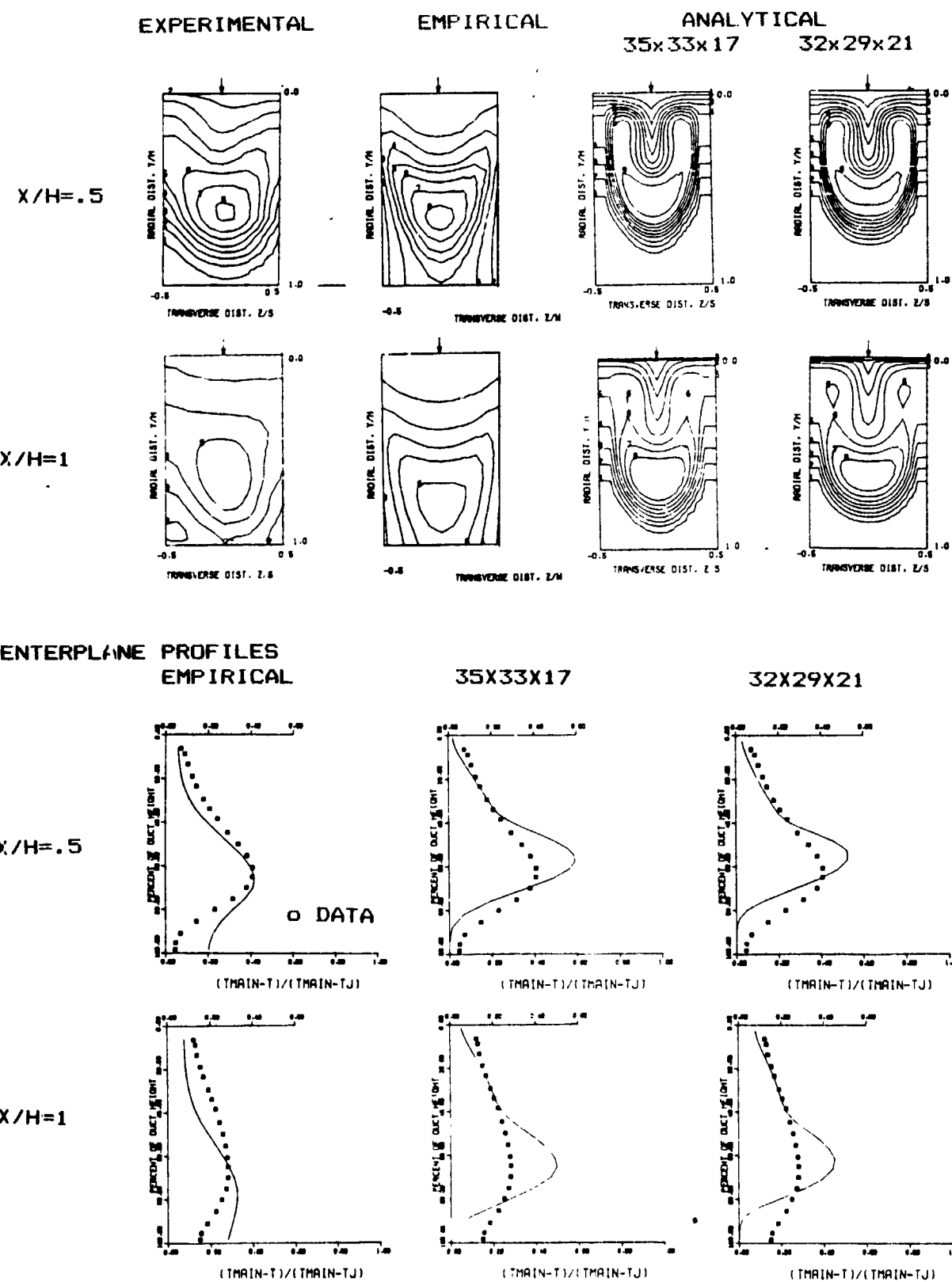
ORIGINAL PAGE IS  
OF POOR QUALITY



a)  $S/H_0=1$ ,  $H_0/D=4$ ,  $A_s/A_0=.049$ ,  $J=5.3$ ,  $w_s/w_T=.107$

Figure 4. Temperature Distributions with Coupled Spacing and Momentum Flux Ratio.

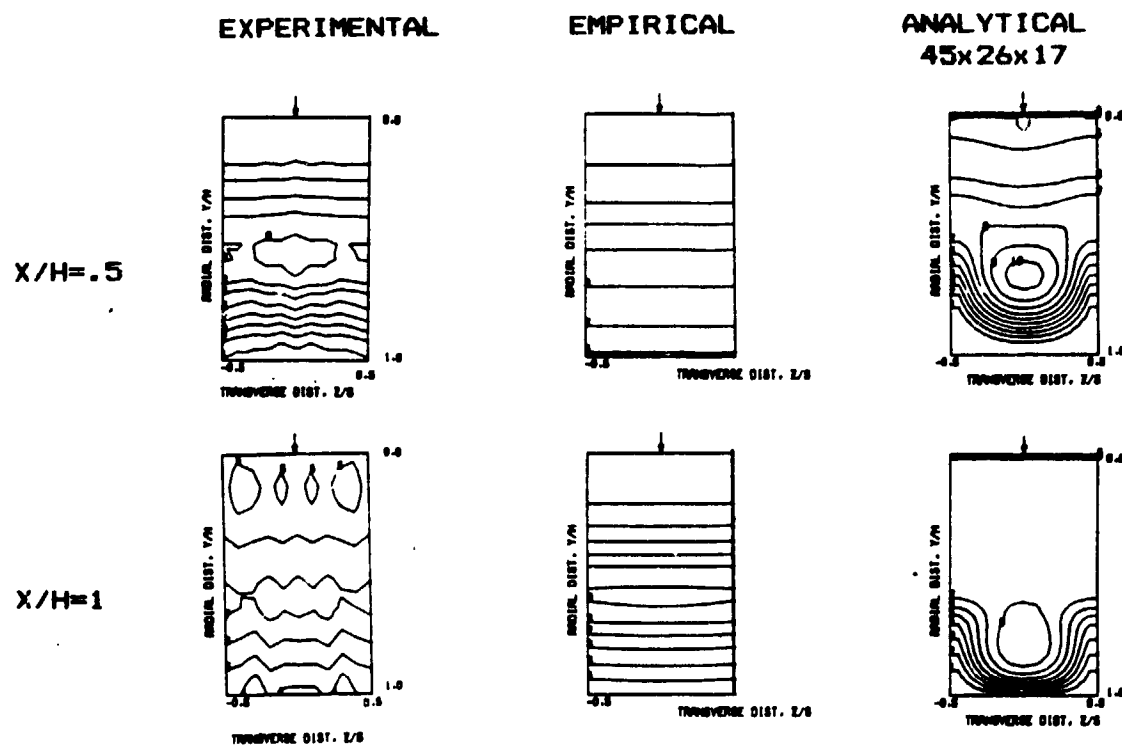
ORIGINAL PAGE IS  
OF POOR QUALITY



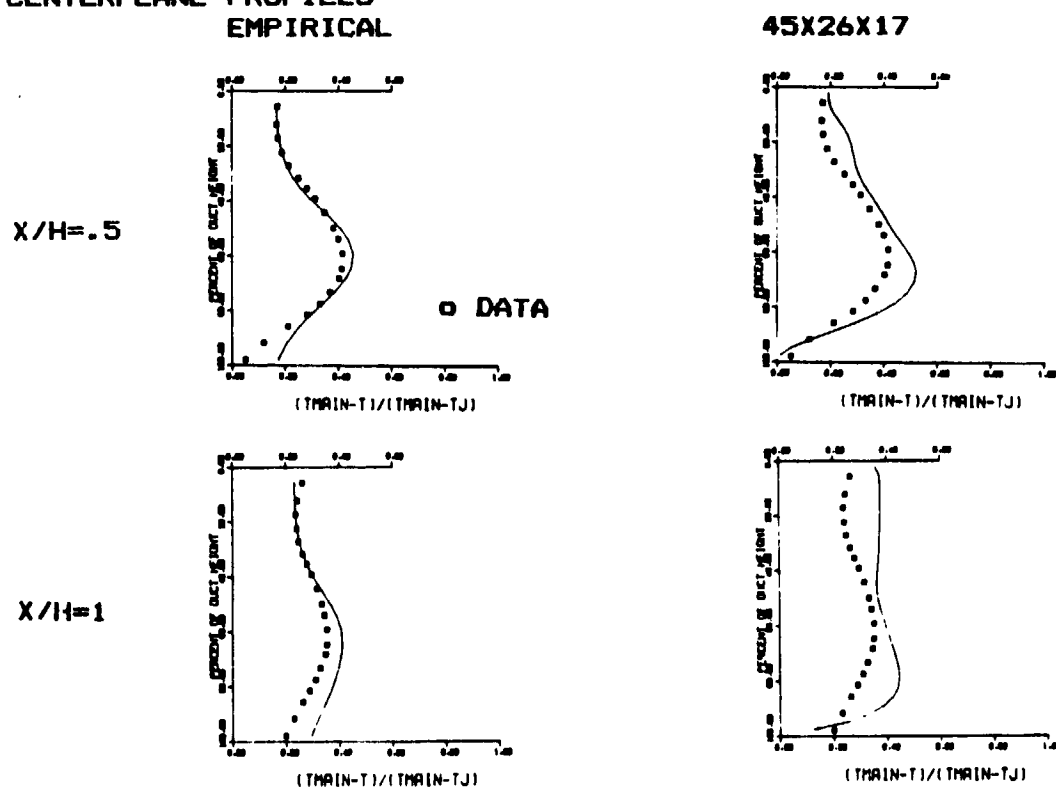
b)  $S/H_0 = .5$ ,  $H_0/D = 5.66$ ,  $A_e/A_0 = .049$ ,  $J = 25.5$ ,  $W_e/W_T = .205$

Figure 4. Temperature Distributions with Coupled Spacing and Momentum Flux Ratio.

ORIGINAL DRAWING  
OF FIGURE 4



CENTERPLANE PROFILES  
EMPIRICAL



c)  $S/H_0 \approx .25$ ,  $H_0/D=8$ ,  $A_s/A_m \approx .049$ ,  $J=92.7$ ,  $W_s/W_t \approx .302$

Figure 4. Temperature Distributions with Coupled Spacing and Momentum Flux Ratio.

ORIGINAL PAGE IS  
OF POOR QUALITY

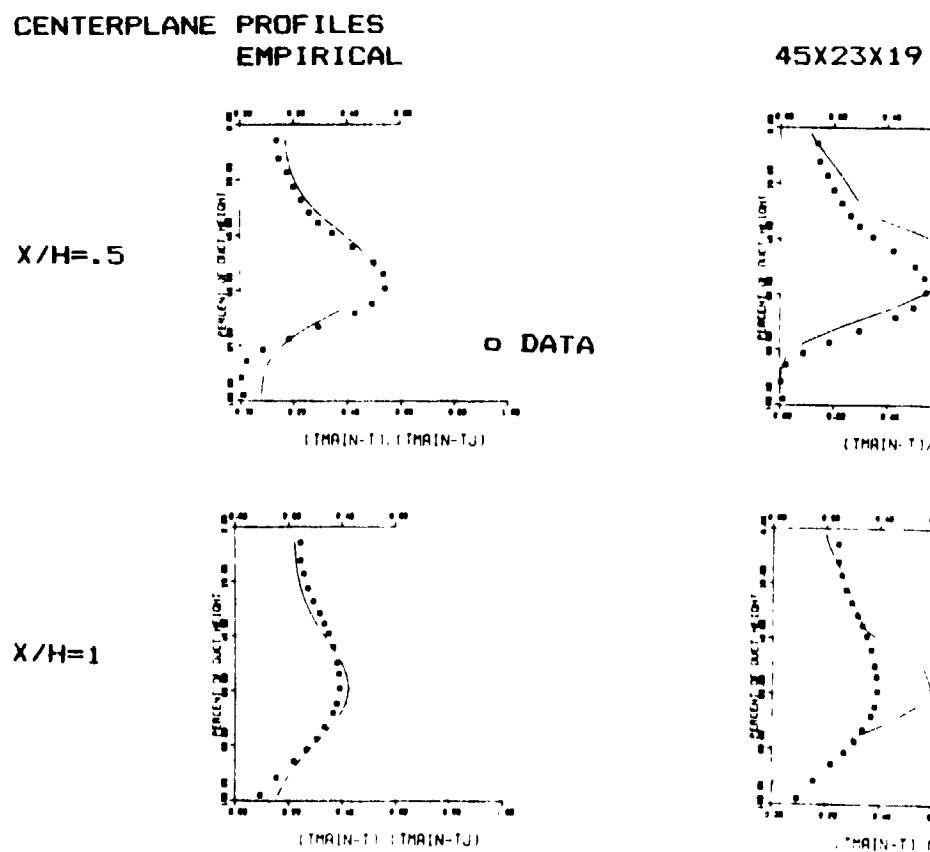
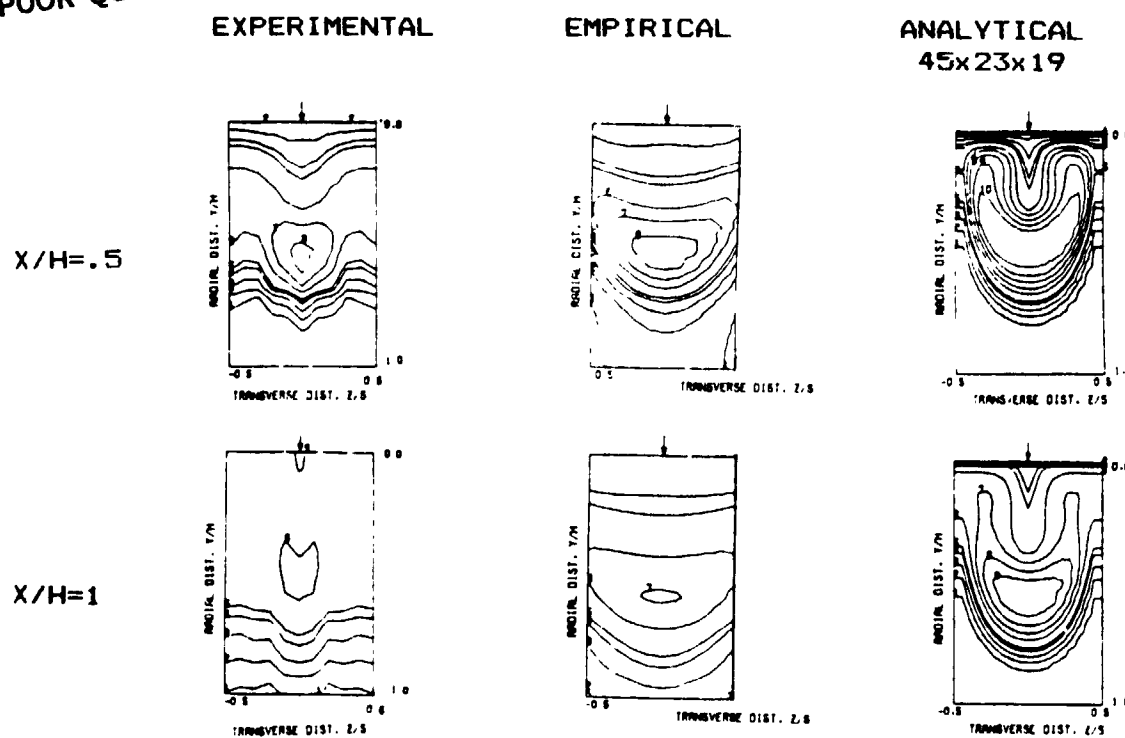
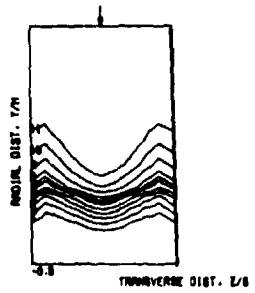


Figure 5. Temperature Distributions for Single-side (top) Injection into an Isothermal Mainstream  
( $S/H_0 = .5$ ,  $H_0 = 4$ ,  $A_r/A_m = .098$ ,  $J = 18.6$ ,  $w_r/w_T = .71$ )

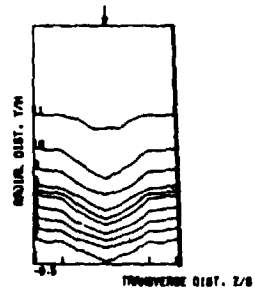
ORIGINAL PAGE IS  
OF POOR QUALITY

EXPERIMENTAL

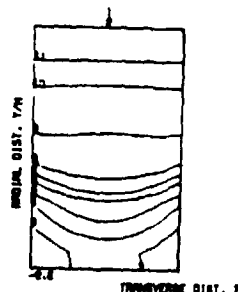
$X/H = .5$



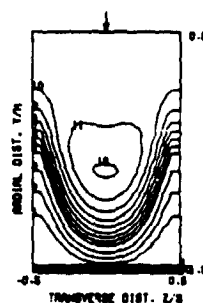
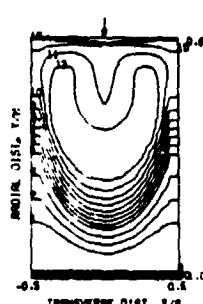
$X/H = 1$



EMPIRICAL

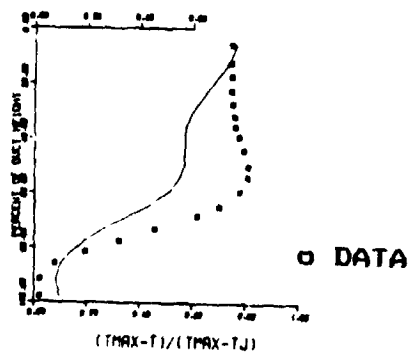


ANALYTICAL  
 $45 \times 23 \times 19$

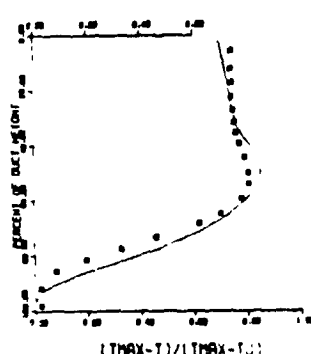


CENTERPLANE PROFILES  
EMPIRICAL

$X/H = .5$



$45 \times 23 \times 19$



$X/H = 1$

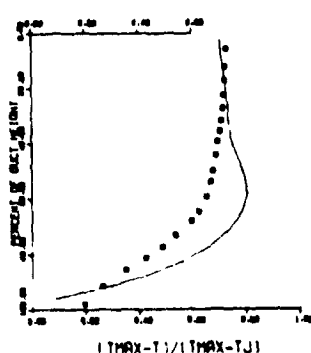
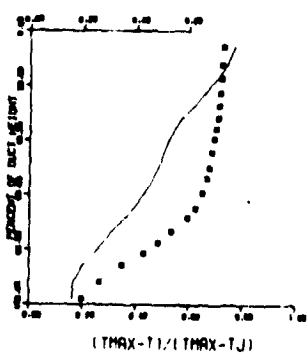
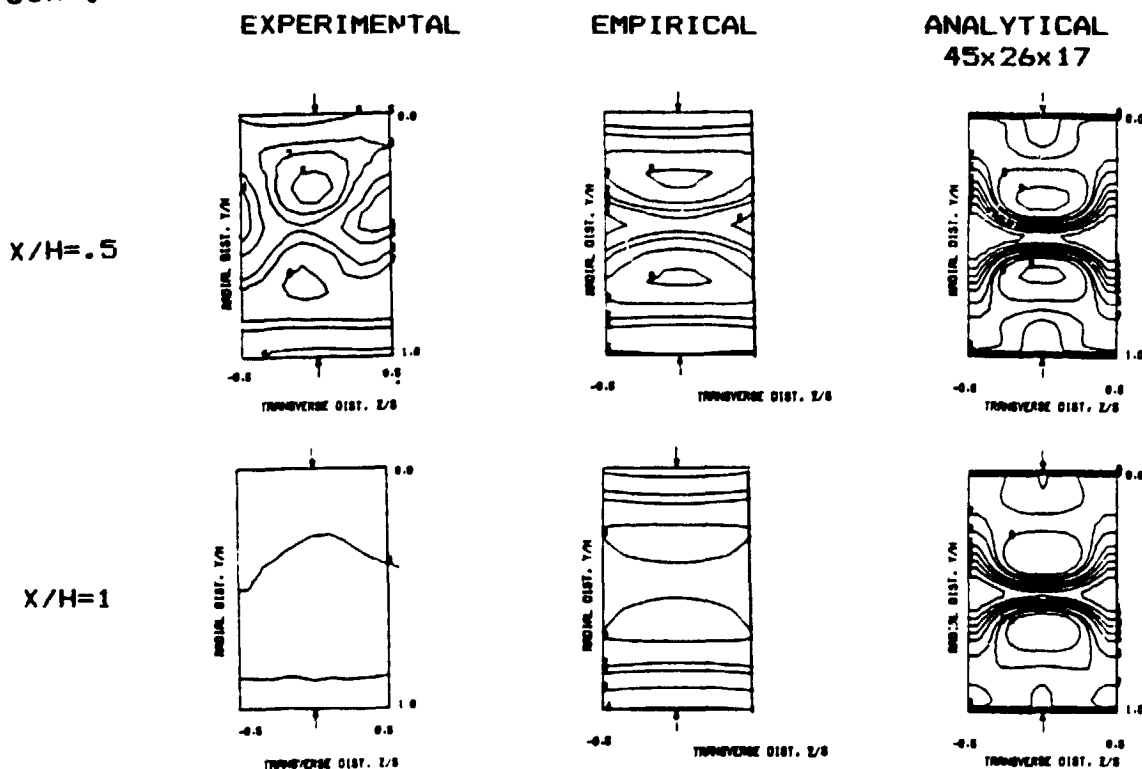


Figure 6. Temperature Distributions for Variable Temperature (Top Cold) Mainstream ( $S/H_0 = .5$ ,  $H_0/D = 4$ ,  $A_s/A_m = .098$ ,  $J = 31.3$ )

ORIGINAL PAGE IS  
OF POOR QUALITY



CENTERPLANE PROFILES  
EMPIRICAL

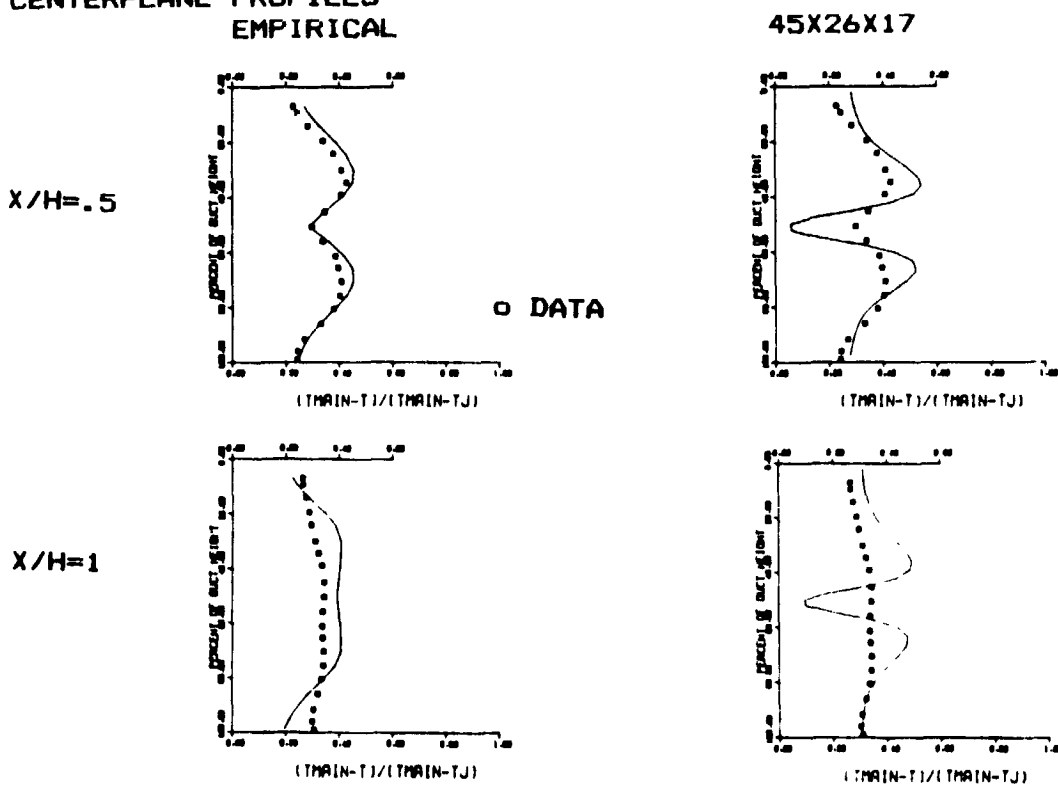
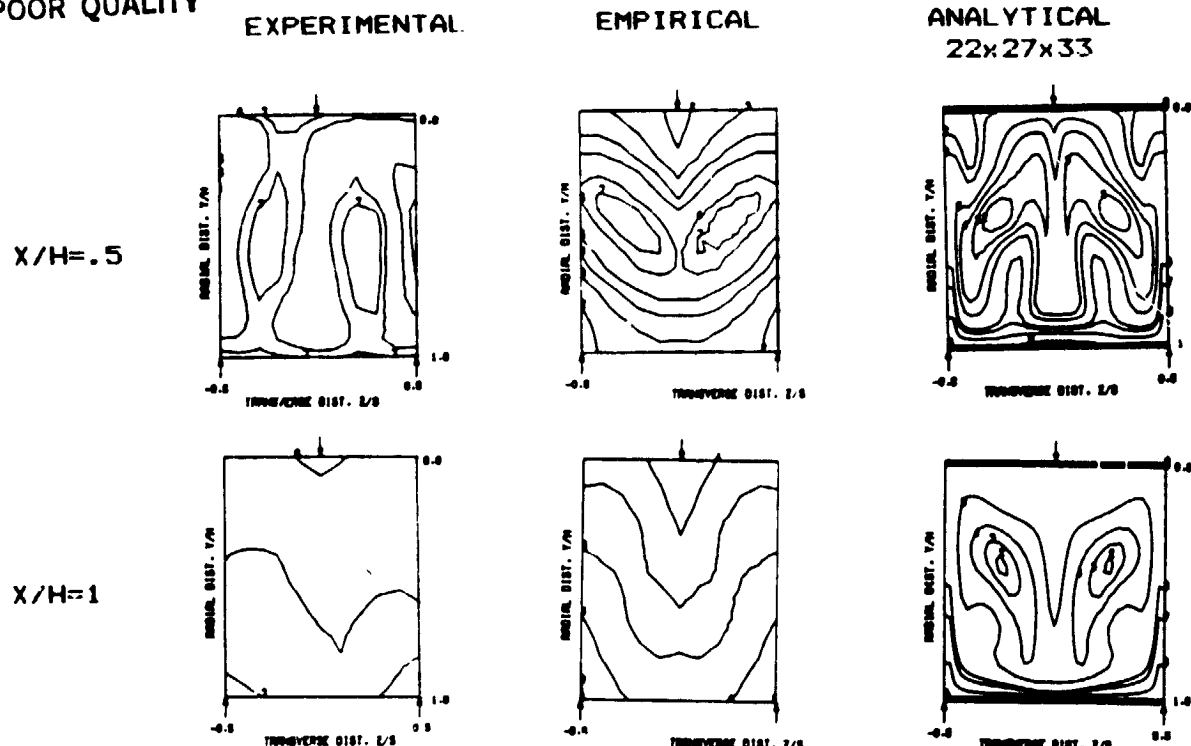


Figure 7. Temperature Distributions for Two-side (opposed) Injection  
( $S/H_0 = .25$ ,  $H_0/D = 8$ ,  $A_s/A_0 = .98$ ,  $J = 25.0$ ,  $W_s/W_0 = .318$ )

ORIGINAL PAGE IS  
OF POOR QUALITY



CENTERPLANE PROFILES  
EMPIRICAL       $22 \times 27 \times 33$

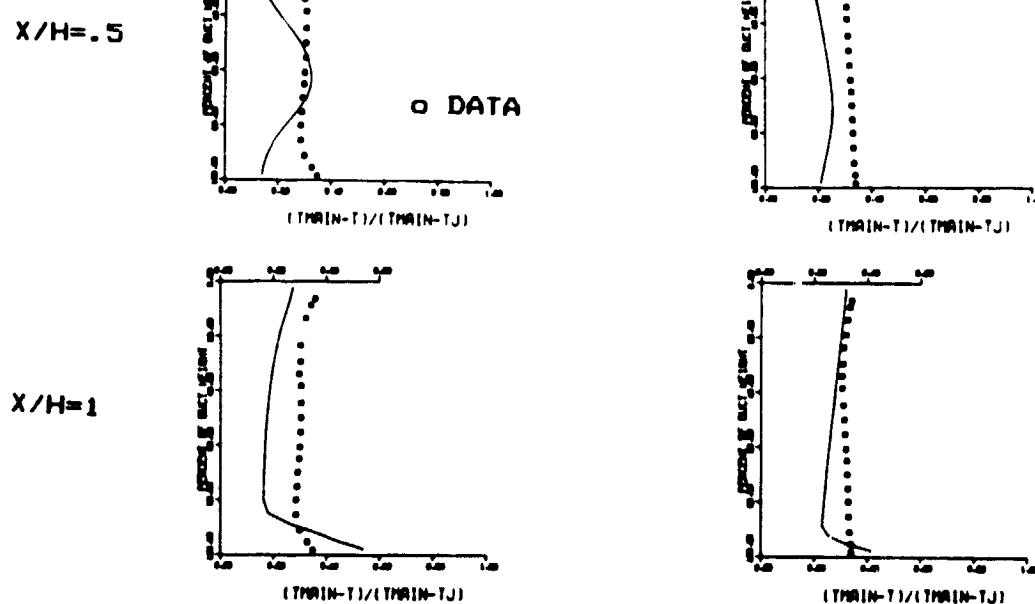


Figure 8. Temperature Distributions for Two-side (staggered) Injection  
( $S/H_0=1$ ,  $H_0/D=4$ ,  $A_s/A_0=.098$ ,  $J=27.6$ ,  $u_s/u_T=.327$ )